Prognostic value of des-γ-carboxyprothrombin in patients with AFP-negative HCC treated with TACE

HANYAO SUN[*], WEI YANG[*], WEIZHONG ZHOU, CHUNGAO ZHOU, SHENG LIU, HAIBIN SHI and WEI TIAN

Department of Interventional Radiology, The First Affiliated Hospital of Nanjing Medical University,
Nanjing, Jiangsu 210029, P.R. China

Abstract. In patients with AFP-negative hepatocellular carcinoma (HCC), des-γ-carboxyprothrombin (DCP) is an important prognostic indicator for the preoperative assessment of transarterial chemoembolization (TACE). However, the association between the serum DCP levels and the degree of progression and prognosis of patients with AFP-negative HCC treated with TACE has not been thoroughly investigated to date, and the molecular mechanism is also unclear. The present study retrospectively analyzed the clinical data of 107 patients with AFP-negative HCC treated with TACE and divided them into two groups based on the median serum DCP levels. The association between DCP and the clinical characteristics of the patients was analyzed, and the survival data were analyzed using Kaplan-Meier curves and Cox regression models. The results demonstrated that the median follow-up time was 755 days (range, 64-1,556 days), and patients in the low-DCP group (n=11; 20.8%) had a lower mortality rate than those in the high-DCP group (n=20; 37.0%). Cox multivariate regression analysis suggested that preoperative lymph node metastasis [hazard ratio (HR), 3.903; 95% CI, 1.778-8.519; P=0.001] and DCP group (HR, 2.465; 95% CI, 1.038-5.854; P=0.041) were independent risk factors. Furthermore, the Gene Expression Omnibus database was utilized to screen differentially expressed mRNAs. Enrichment analyses were then performed, and a protein-protein interaction (PPI) network was constructed to identify hub genes. A total of 169 differentially expressed genes were screened. Enrichment analyses revealed that cancer-related and ribosomal pathways were significantly enriched. Furthermore, 10 hub genes were identified in the PPI network by counting the number of gene interactions, the majority of which belonged to the ribosomal protein (RPS) family, and the top three significant genes were RPS23, RPS11 and RPS3A. In patients with AFP-negative HCC, higher serum DCP levels were associated with poor prognosis after TACE. This may be associated with genes such as those belonging to the RPS family, which may contribute to future personalized therapy for this disease.

Introduction

Hepatocellular carcinoma (HCC) is one of the most common malignant tumors, ranking sixth in incidence worldwide, and is the fourth leading cause of cancer-associated mortality, with a 5-year survival rate of only 18% (1,2). Furthermore, the onset of HCC is insidious, and there are no obvious clinical symptoms at the early stage (2). The majority of HCC cases are diagnosed at advanced stages, and are ineligible for curative resection, which leads to poor prognosis (2). Transarterial chemoembolization (TACE) is one of the most effective treatments for patients with unresectable HCC worldwide (3-5). HCC obtains its blood supply mainly from the hepatic artery, which provides 90% of the blood supply (6). In TACE, direct delivery of drugs to the tumor by intra-arterial chemotherapy, during which liver blood flow is occluded, is often used to induce ischemia and hypoxia of the tumor tissue, which leads to long-term retention of the drug to enhance the subsequent necrosis (7). However, HCC exhibits remarkable cellular heterogeneity, which contributes to high rates of therapeutic resistance and rapid recurrence (8,9). A total of 27 randomized controlled trials between 1978 and 2002 suggested that the objective response rate for TACE was only 15-55% and that 70-80% of patients treated with TACE would die from tumor progression rather than liver failure (10,11). Therefore, the relatively high incidence of tumor recurrence after TACE suggests that adequate assessment of its therapeutic efficacy and prognosis is required before TACE.

Serum-based tumor biomarkers are widely used to predict tumor prognosis preoperatively, and AFP is the most common one in HCC (12). However, due to tumor heterogeneity, certain patients with AFP-negative HCC require novel tumor biomarkers for the prediction of their prognosis in clinical

Correspondence to: Dr Haibin Shi or Dr Wei Tian, Department of Interventional Radiology, The First Affiliated Hospital of Nanjing Medical University, 300 Guangzhou Road, Nanjing, Jiangsu 210029, P.R. China
E-mail: shihb@njmu.edu.cn
E-mail: tianwei@jsph.org.cn

[*]Contributed equally

settings (13). A recent study noted that ~50% of patients with HCC are AFP-negative, particularly those at an early stage and with small HCC tumors (14). Des-γ-carboxyprothrombin (DCP) was first proposed by Liebman *et al* (15) in 1984. It has been reported that DCP has a higher value in the evaluation of HCC than AFP (12,15). The presence of ≥1 glutamate residues in the γ-carboxyglutamic acid-rich structural domain that are not fully carboxylated to γ-carboxyglutamate leads to the synthesis of the aforementioned immature thrombin by the liver (16). DCP has been reported to be elevated in patients with HCC (12,13). To the best of our knowledge, for patients with 'single-positive' HCC (AFP-negative and DCP-positive), the association between the level of DCP and the therapeutic efficacy and prognosis of TACE remains unclear. In addition, the key signaling pathways, hub genes and potential molecular mechanisms involved in the pathology of these patients remain to be identified.

The present study retrospectively reviewed the clinical data of patients with 'single-positive' HCC, aiming to explore the role of DCP in the therapeutic efficacy and prognosis of TACE. Differentially expressed genes (DEGs) between HCC and normal tissues were obtained from a microarray dataset in the Gene Expression Omnibus (GEO) database. Subsequently, Gene Ontology (GO) analysis, Kyoto Encyclopedia of Genes and Genomes (KEGG) analysis and Gene Set Enrichment Analysis (GSEA) were performed, followed by protein-protein interaction (PPI) network analysis based on these DEGs. The combination of clinical survival analysis and bioinformatics methods may provide novel insights for clinical treatments and drug target discovery in HCC.

Materials and methods

Ethics. The present retrospective study was approved by the ethics committee review board of Jiangsu Provincial Hospital (Nanjing, China), which waived the requirement for informed patient consent (approval no. 2022-SR-249). All the procedures performed in the present study were consistent with the ethical standards of institutional and national research committees, and with the 1964 Declaration of Helsinki and its later amendments or comparable ethical standards. The authors could identify the information of individual participants only during data collection. A flowchart of the present study is shown in Fig. 1.

Patient selection. The medical records of 634 consecutive adult patients with HCC treated with TACE as the initial treatment between December 2016 and February 2021 at the Department of Interventional Radiology, The First Affiliated Hospital of Nanjing Medical University (Nanjing, China) were analyzed in the present study. The patients were diagnosed with HCC based on clinical symptoms, serological tests, imaging and pathological evaluations according to the 'Primary Liver Cancer Clinical Diagnosis and Staging Criteria' (17). The 107 patients who met the inclusion criteria were included in the analysis and were divided into low-DCP (≤180 mAU/ml) and high-DCP (>180 mAU/ml) groups according to the median serum levels of DCP (Table SI). The inclusion criteria were as follows: i) Patients were aged between 18 and 85 years; ii) Eastern Cooperative Oncology Group (ECOG) (18)

performance status of 0-2; iii) no ability to accept curative surgery, such as partial hepatectomy; iv) preoperative serum AFP was negative (<20.00 ng/ml); and v) serum DCP was positive (≥40 mAU/ml). The exclusion criteria were as follows: i) Diffuse-type HCC; ii) ECOG performance score >2; iii) decompensated cirrhosis; iv) patients with severe heart, liver, brain, lung, kidney, hematopoietic system and neuropsychiatric disorders; and v) presence of any other malignancy. All patients were observed until mortality or end of follow-up in May 2021.

Standard conventional-TACE procedure. The TACE procedure began with routine disinfection, followed by towel spreading and administration of local anesthesia with 2% lidocaine. A 5-F sheath was introduced into each patient's femoral artery using the Seldinger technique (19), and a 5-F RH catheter (Terumo Corporation) was then used, through which arteriography of the celiac trunk, superior mesenteric artery and hepatic arteries was successively performed to collect an overview of the hepatic arterial blood supply and to evaluate the location, number and size of HCC tumors. A 2.7-F microcatheter (Terumo Corporation) was employed for superselection of the blood supply artery, and angiography confirmed that the microcatheter was accurately positioned. Once the target artery was catheterized, a 1:1 mixed suspension of iodized oil (1-10 ml; Lipiodol Ultra-Fluide; Yantai Luyin Pharmaceutical Co., Ltd.) and epirubicin (20-40 mg; Pharmorubicin; Pfizer, Inc.) was infused into the artery through the catheter, depending on liver function and tumor size. Finally, gelatin sponge particles (Gelfoam; Jiangxi Xiangen Medical Technology Development Co., Ltd.) were infused to embolize the artery until no tumor staining was found after repeated angiography. Finally, the guidewire and catheters were removed, and the femoral artery was compressed for 10 min to secure hemostasis at the puncture site.

Clinical data. The patients' demographic data, results of serological tests, imaging results, survival data and clinical manifestations were collected from medical records, and the Child-Pugh classification and ECOG score were also assessed (20,21). Routine laboratory analyses included hematology screening, blood chemistry panel, coagulation function tests, liver function tests and tumor markers (including AFP and DCP). All patients were subjected to abdominal CT or MRI examination to determine the tumor number and size, and to establish whether there was metastasis. Patients were followed up by telephone and outpatient review. The first follow-up visit was in the first month after surgery; thereafter, follow-up was every 3 months in the first year after surgery, every 6 months in the second and third years after surgery, and annually thereafter. The overall survival (OS) time was defined as the time interval from the date of surgery to the end of follow-up or mortality date (Table SI).

Microarray data. mRNA expression profiles were downloaded from the GEO (22) platform GPL16699-Agilent-039494 SurePrint G3 Human GE v2 8x60K Microarray 039381 (Feature Number version) (GSE57555), which included 16 tumor tissues and 16 nontumor tissues (23). A total of 3 tumor tissues (GSM1384684, GSM1384688 and GSM1384690)
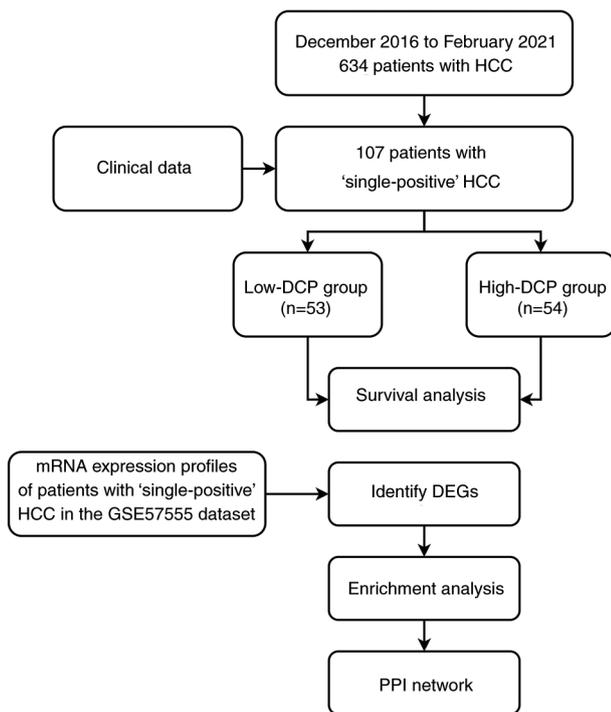
Figure 1. Flowchart of the present study. DCP, des-γ-carboxyprothrombin; DEGs, differentially expressed genes; HCC, hepatocellular carcinoma; PPI, protein-protein interaction.

and 3 nontumor tissues (GSM1384685, GSM1384689 and GSM1384691) from patients with 'single-positive' HCC were selected for analysis.

Identification of DEGs. The downloaded platform and matrix files were converted using R software (version 4.1; www.r-project.org/). Probes were converted to gene symbols according to the platform annotation information of the normalized data. Probes with >1 gene were eliminated, and the mean value was calculated for genes corresponding to >1 probe. The limma package version 3.40.2 of R software (24) was used to study the differential expression of mRNAs. P<0.05 and |log2 fold change|>1 were defined as the threshold criteria to identify the final DEGs. Heatmaps and volcano plots of DEGs were generated using the pheatmap version 1.0.12 (https://CRAN.R-project.org/package=pheatmap) and ggplot2 version 3.3.0 (https://CRAN.R-project.org/package=ggplot2) packages.

Functional enrichment analysis of DEGs. To identify the affected biological processes, the Bioconductor package 'Cluster Profiler' (version 4.4.0; https://bioconductor.org/pack-ages/release/bioc/html/clusterProfiler.html) of R software was used to classify the enriched GO terms (http://geneontology.org/). Information in the KEGG database (https://www.kegg.jp/) was used for the pathway enrichment analysis of DEGs. P<0.05 indicated a statistically significant selection of GO terms and KEGG pathways (25).

GSEA. GSEA was carried out for all genes that were also detected using the package 'Cluster Profiler' in R. The genes were sorted according to their expression and compared with

the KEGG database to provide another option for screening possible differential biological functions. The gene set arrangement was performed 1,000 times per analysis. Gene sets were considered to be significantly enriched with an α or P-value <0.05 and a false discovery rate <25%.

PPI network of DEGs. PPI networks of DEGs were constructed utilizing the Search Tool for the Retrieval of Interacting Genes/Proteins (STRING) database (version 11.5) (26), and were visualized using Cytoscape software (version 3.8.2; https://cytoscape.org/), the cytoHubba plugin (27) and the MCODE plugin (28). From 787,896 pairs of human protein interactions containing 16,730 genes, DEG-containing interactions were obtained. STRING utilized a combined score from 0 to 1 to assess reliability. Each protein was regarded as a node in the network, and the degree of a node was considered to be the number of interactions with other nodes. Hub genes were nodes with ≥50 degrees.

Statistical analysis. Statistical analysis was conducted using SPSS 26.0 for Windows (IBM Corp.) and R software version 4.1 (www.r-project.org/). Continuous data are presented as the mean ± standard deviation or as the median (interquartile range). Unpaired Student's t-test was used to determine differences in continuous variables that followed a normal distribution between two groups. Non-normally distributed data were compared using U-Mann Whitney test. Non-continuous and categorical data were compared with c^2 test and Fisher's test. For survival analysis, the Kaplan-Meier method was applied. For comparisons of survival between groups, the log-rank test was employed. Univariate analysis was performed with the Cox regression model, and variables with P≤0.1 in univariate analysis were included in the multivariate Cox regression model. P<0.05 was considered to indicate a statistically significant difference.

Results

Baseline patient demographics and clinical characteristics. The demographic and baseline characteristics of our study cohort are shown in Table I. A total of 107 patients, 53 in the low-DCP group and 54 in the high-DCP group, were included in the study. They did not significantly differ in age (P=0.745), sex (P=0.356), hepatitis (P=0.784), Child-Pugh classification (P=0.322), aspartate transaminase (AST; P=0.126), total bilirubin (TBil; P=0.660), high-density lipoprotein (HDL; P=0.079), retinol binding protein (RBP; P=0.843), platelet count (PLT; P=0.429), plateletcrit (PCT; P=0.198), platelet distribution width (PDW; P=0.571), red cell distribution width (RDW; P=0.625), tumor number (P=0.126), lymphatic node metastasis (P=0.113) or distant metastasis (P>0.999) (Table I). The results indicated that patients in the two groups were comparable. Nevertheless, significant differences in ECOG score (P=0.043), alanine transaminase (ALT; P=0.037) and tumor size (P<0.001) were observed.

Comparison of prognosis between the low-DCP group and the high-DCP group. In our cohort, the median follow-up time of all patients was 755 days (64-1,556 days); 31 patients died, 75 survived and 1 was lost to follow-up. 11 patients in

Table I. Baseline demographic data and characteristics of the patients in our cohort.

Variables	All patients (n=107)	Low-DCP group (n=53)	High-DCP group (n=54)	Statistical value	P-value
Age, n (%)				χ^2=0.106	0.745
>60 years	40 (37.4)	19 (35.8)	21 (38.9)		
≤60 years	67 (62.6)	34 (64.2)	33 (61.1)		
Sex, n (%)				χ^2=0.853	0.356
Male	94 (87.9)	45 (84.9)	49 (90.7)		
Female	13 (12.1)	8 (15.1)	5 (9.3)		
Hepatitis, n (%)				χ^2=0.075	0.784
Yes	72 (67.3)	35 (66.0)	37 (68.5)		
No	35 (32.7)	18 (34.0)	17 (31.5)		
ECOG score, n (%)				χ^2=4.114	0.043
0	50 (46.7)	30 (56.6)	20 (37.0)		
1	57 (53.3)	23 (43.4)	34 (63.0)		
Child-Pugh classification, n (%)				χ^2=0.981	0.322
A	89 (83.2)	46 (86.8)	43 (79.6)		
B	18 (16.8)	7 (13.2)	11 (20.4)		
ALT, U/l	26.9 (19.3-42.2)	23.9 (18.2-32.6)	31.4 (20.4-50.0)	U=1765.5	0.037
AST, U/l	33.9 (26.1-45.2)	32.3 (25.0-40.7)	34.8 (26.5-53.0)	U=1676.5	0.126
TBil, μmol/l	15.1 (11.2-22.3)	14.7 (11.1-22.4)	16.3 (11.3-22.4)	U=1501.5	0.660
HDL, mmol/l	1.08±0.3	1.14±0.3	1.03±0.3	t=1.774	0.079
RBP, mg/l	23.9±10.1	23.7±9.9	24.1±10.3	t=-0.199	0.843
PLT, 10^9/l	137.9±70.1	132.4±70.4	143.3±70.0	t=-0.798	0.429
PCT, %	14.5±7.2	13.6±7.2	15.4±7.1	t=-1.296	0.198
PDW, %	16.0 (13.7-17.2)	16.0 (13.6-17.1)	16.0 (13.8-17.1)	U=1522.0	0.571
RDW, %	13.6 (13.0-14.9)	13.7 (12.9-15.3)	13.6 (13.0-14.7)	U=1352.5	0.625
Tumor size, cm	3.35 (2.2-6.7)	2.6 (1.9-4.9)	4.4 (2.8-8.1)	U=1974.0	<0.001
Tumor number, n (%)				χ^2=2.341	0.126
Single	33 (30.8)	20 (37.7)	13 (24.1)		
Multiple	74 (69.2)	33 (62.3)	41 (75.9)		
N-metastasis, n (%)				χ^2=2.256	0.113
Yes	27 (25.2)	10 (18.9)	17 (31.5)		
No	80 (74.8)	43 (81.1)	37 (68.5)		
M-metastasis, n (%)					>0.999
Yes	3 (2.8)	1 (1.9)	2 (3.7)		
No	104 (97.2)	52 (98.1)	52 (96.3)		

Continuous data are presented as the mean ± standard deviation (HDL, RBP, PLT and PCT) or as the median (interquartile range) (ALT, AST, TBil, PDW, RDW and tumor size). Unpaired Student's t-test was used to determine differences in continuous variables that followed a normal distribution between two groups. Non-normally distributed data were compared using U-Mann Whitney test. Non-continuous and categorical data were compared with the χ^2 test (age, sex, hepatitis, ECOG score, Child-Pugh classification, tumor number and N-metastasis) and Fisher's test (M-metastasis). ALT, alanine transaminase; AST, aspartate transaminase; DCP, des-γ-carboxyprothrombin; ECOG, Eastern Cooperative Oncology Group; HDL, high-density lipoprotein; PCT, plateletcrit; PDW, platelet distribution width; PLT, platelet count; RBP, retinol binding protein; RDW, red cell distribution width; TBil, total bilirubin.

the low-DCP group (20.8%) died. Among them, 10 died from HCC progression and 1 died from other causes. In addition, 20 patients in the high-DCP group (37.0%) died, all from HCC progression. The mean survival time in the low-DCP group was 1,350 days, whereas the mean survival time in the high-DCP group was 1,005 days. The median survival time in the high-DCP group was 1,079 days, and the median survival time in the low-DCP group was not reached. Survival analysis was performed using the Kaplan-Meier method with a log-rank test. The OS time of the patients in the high-DCP group was shorter than that of the patients in the low-DCP group (log-rank P=0.0022; Fig. 2).
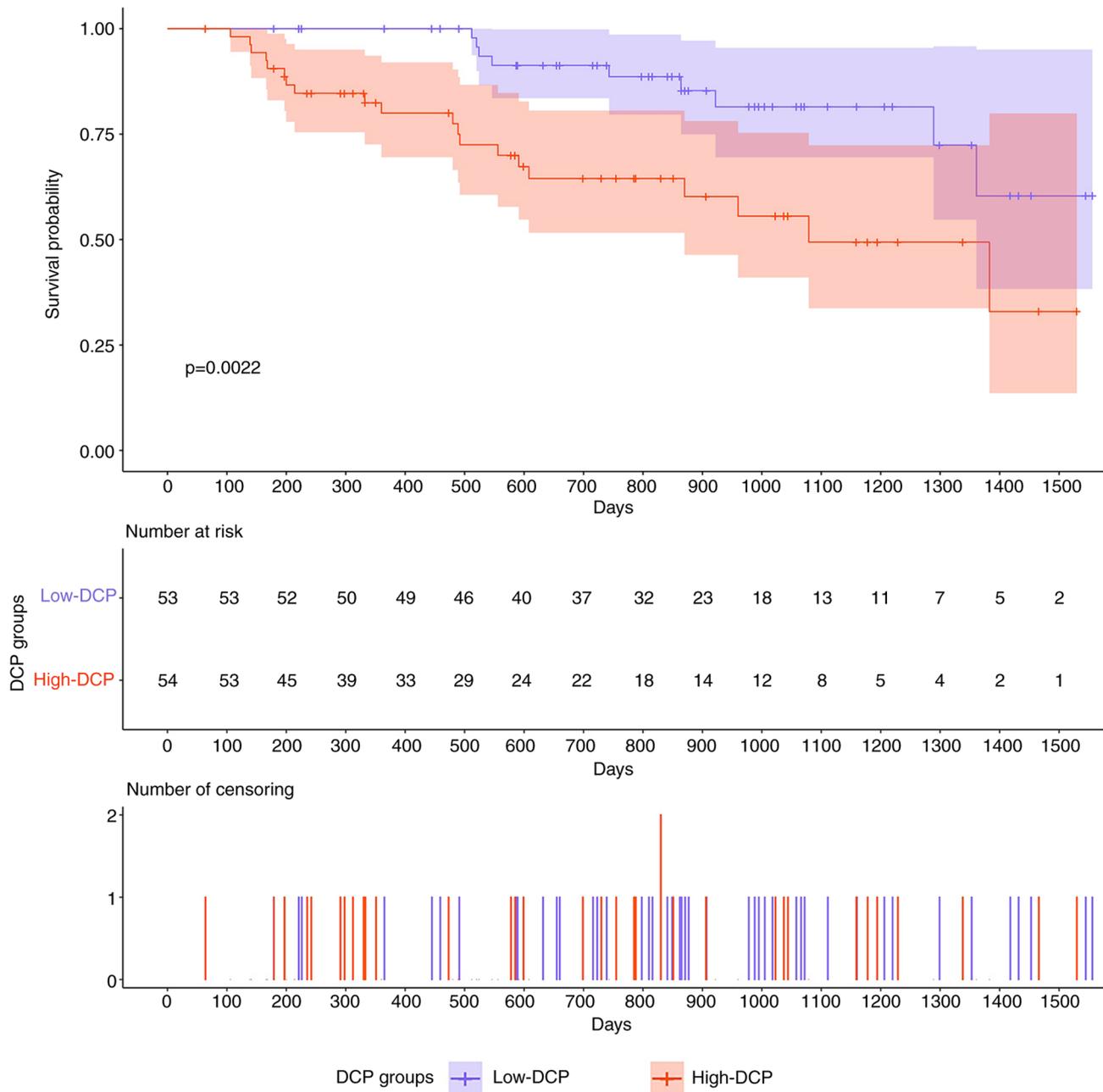
Figure 2. Kaplan-Meier survival curves of our cohort. Comparison of Kaplan-Meier overall survival curves revealed that the low-DCP group had a longer postsurgical survival time. DCP, des-γ-carboxyprothrombin.

Prognostic factors of 'single-positive' patients who underwent TACE. In univariate analysis of OS time, lymphatic node metastasis [hazard ratio (HR), 3.924; P<0.001; 95% CI, 1.883-8.181], DCP group (HR, 3.219; P=0.004; 95% CI, 1.461-7.093), Child-Pugh classification (HR, 2.876; P=0.010; 95% CI, 1.287-6.427), tumor size (HR, 1.085; P=0.026; 95% CI, 1.010-1.167), tumor number (HR, 3.061; P=0.038; 95% CI, 1.062-8.822) and HDL (HR, 0.265; P=0.048; 95% CI, 0.071-0.991) were significant prognostic factors in our cohort. In multivariate analysis of OS time, lymphatic node metastasis (HR, 3.903; P=0.001; 95% CI, 1.778-8.519) and DCP group (HR, 2.465; P=0.041; 95% CI, 1.038-5.854) were significant prognostic factors of poor survival. The results are shown in Table II.

Identification of DEGs in 'single-positive' patients. To identify DEGs in tumor tissues and normal tissues of 'single-positive' patients, the mRNA expression profile dataset (GSE57555) from 'single-positive' patients with HCC was first downloaded. Based on the cutoff criteria used to determine the DEGs, 169 DEGs were identified between tumor and nontumor samples (adjacent tumor tissues from the same patients), including 83 upregulated DEGs and 86 downregulated DEGs. A volcano plot (Fig. 3A) and a clustering heatmap (Fig. 3B) indicated the distribution of DEGs.

GO and KEGG pathway enrichment analyses of DEGs. Next, it was attempted to identify the biological function of the 169 DEGs. The Bioconductor package 'Cluster Profiler' of

Table II. Univariate and multivariate analyses of prognostic factors for overall survival of patients in our cohort.

Variables	Univariate analysis		Multivariate analysis	
	HR (95% CI)	P-value	HR (95% CI)	P-value
Age (≤60 vs. >60 years)	1.614 (0.714-3.648)	0.250		
Sex (male vs. female)	0.521 (0.211-1.284)	0.157		
DCP group (low-DCP group vs. high-DCP group)	3.219 (1.461-7.093)	0.004	2.465 (1.038-5.854)	0.041
Hepatitis (yes vs. no)	0.725 (0.334-1.574)	0.416		
ECOG score (0 vs. 1)	1.762 (0.816-3.808)	0.149		
Child-Pugh classification (A vs. B)	2.876 (1.287-6.427)	0.010	1.887 (0.798-4.459)	0.148
ALT	1.011 (0.995-1.026)	0.181		
AST	1.009 (0.994-4.024)	0.229		
TBil	1.008 (1.000-1.017)	0.061		
HDL	0.265 (0.071-0.991)	0.048	0.743 (0.198-2.782)	0.659
RBP	1.002 (0.966-4.040)	0.913		
PLT	1.004 (0.999-4.009)	0.168		
PCT	1.029 (0.980-4.081)	0.248		
PDW	0.963 (0.829-4.120)	0.627		
RDW	0.966 (0.810-4.152)	0.700		
Tumor size	1.085 (1.010-1.167)	0.026	1.062 (0.975-1.158)	0.170
Tumor number (single vs. multiple)	3.061 (1.062-8.822)	0.038	2.402 (0.811-7.111)	0.114
N-metastasis (yes vs. no)	3.924 (1.883-8.181)	<0.001	3.903 (1.778-8.519)	0.001
M-metastasis (yes vs. no)	0.704 (0.095-5.217)	0.731		

Age, sex, DCP group, hepatitis, ECOG score, Child-Pugh classification, tumor number N-metastasis and M-metastasis were analyzed as categorical variables, and ALT, AST, TBil, HDL, RBP, PLT, PCT, PDW, RDW and tumor size were analyzed as a continuous variable. ALT, alanine transaminase; AST, aspartate transaminase; DCP, des-γ-carboxyprothrombin; ECOG, Eastern Cooperative Oncology Group; HDL, high-density lipoprotein; HR, hazard ratio; PCT, plateletcrit; PDW, platelet distribution width; PLT, platelet count; RBP, retinol binding protein; RDW, red cell distribution width; TBil, total bilirubin.

R software was used to carry out GO functional enrichment analysis.

As shown in Fig. 4 and Table III, the top five terms for biological processes were: 'SRP-dependent cotranslational protein targeting to membrane', 'cotranslational protein targeting to membrane', 'nuclear-transcribed mRNA catabolic process, nonsense-mediated decays', 'protein targeting to ER' and 'establishment of protein localization to the endoplasmic reticulum'. The top two molecular functions were: 'structural constituent of ribosome' and 'rRNA binding'. The top five terms for cellular components were: 'cytosolic ribosome', 'ribosomal subunit', 'ribosome', 'cytosolic large ribosomal subunit' and 'large ribosomal subunit'.

In addition, the results of KEGG pathway enrichment analysis indicated that upregulated DEGs were mainly enriched in the 'Ribosome' and the 'Coronavirus disease-COVID-19' pathway. The top five pathways in terms of significance enriched by the downregulated DEGs include: 'Mineral absorption', 'PPAR signaling pathway', 'Complement and coagulation cascades', 'Valine, leucine and isoleucine degradation' and the 'Arginine biosynthesis' pathway (Fig. 5B and C;

Table IV). Fig. 5A shows the top six pathways that were significantly enriched for all genes.

GSEA. GSEA was performed to identify the potential associated biological processes and signaling pathways. As shown in Fig. 6, several cancer-related and protein synthesis pathways, such as 'Cellular senescence', 'Ribosome' and 'Cell adhesion molecules' pathways, were enriched. The results also showed the enrichment of the 'Human papillomavirus infection' pathway.

PPI network of DEGs. As shown in Fig. 7A, the PPI network based on STRING included 169 DEGs gathered as a cluster consisting of 133 nodes and 1,944 edges. These results were imported into Cytoscape software for visual analysis. Using the cytoHubba plugin and the degree method, the top 10 hub genes were identified: Ribosomal protein (RPS)23, UBA52, RPS11, RPS3A, RPS2, RPS15, RPS5, RPL6, RPL18 and RPS13 (Fig. 7B). In addition, the MCODE plugin of Cytoscape was used to analyze the whole network, which identified seven subnetworks (Fig. 7C). Of these, module 1
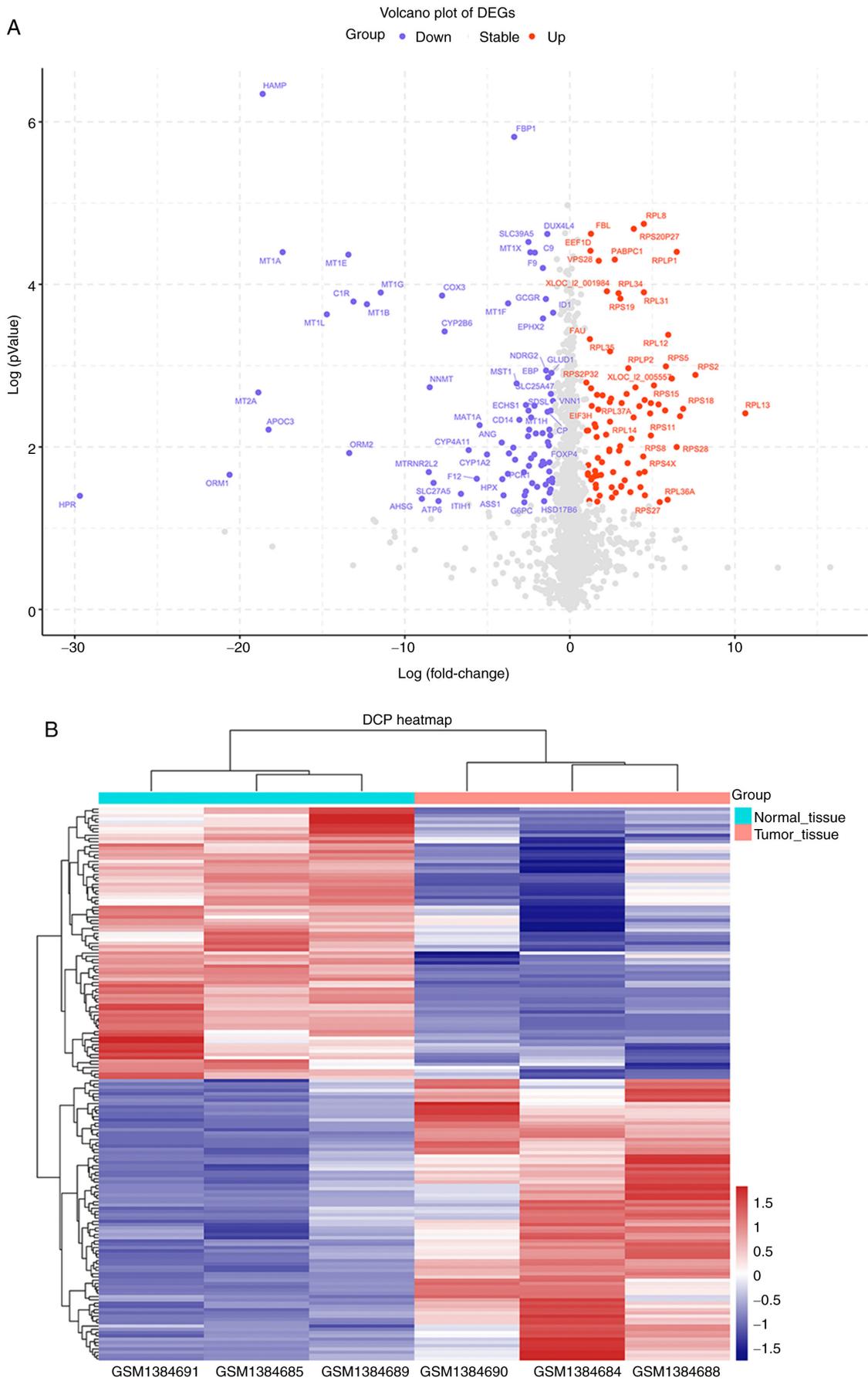
Figure 3. DEGs of 'single-positive' patients extracted from the mRNA expression profile dataset (GSE57555). Volcano plot and heatmap. (A) Volcano plot of DEGs. Data points in red represent upregulated genes, and purple represents downregulated genes. The cut-off value set at the absolute value of log2 fold change >1. (B) Heatmap of differentially expressed genes. The legend on the bottom right indicates the log fold change of the genes. DCP, des-γ-carboxyprothrombin; DEGs, differentially expressed genes.

Table III. Most significantly enriched GO terms for differentially expressed genes determined using the Gene Expression Omnibus dataset.

GO ID	GO name	Gene ratio	P-value
BP			
GO:0006614	SRP-dependent cotranslational protein targeting to membrane	50/151	3.36×10^{-79}
GO:0006613	Cotranslational protein targeting to membrane	50/151	4.03×10^{-78}
GO:0000184	Nuclear-transcribed mRNA catabolic process, nonsense-mediated decay	51/151	1.51×10^{-77}
GO:0045047	Protein targeting to ER	50/151	2.04×10^{-75}
GO:0072599	Establishment of protein localization to endoplasmic reticulum	50/151	1.63×10^{-74}
GO:0070972	Protein localization to endoplasmic reticulum	50/151	4.20×10^{-69}
GO:0006413	Translational initiation	53/151	1.02×10^{-68}
GO:0019083	Viral transcription	51/151	5.91×10^{-67}
GO:0019080	Viral gene expression	51/151	1.22×10^{-64}
GO:0000956	Nuclear-transcribed mRNA catabolic process	51/151	8.67×10^{-63}
CC			
GO:0022626	Cytosolic ribosome	52/152	6.65×10^{-83}
GO:0044391	Ribosomal subunit	52/152	3.55×10^{-68}
GO:0005840	Ribosome	53/152	1.32×10^{-60}
GO:0022625	Cytosolic large ribosomal subunit	30/152	6.05×10^{-49}
GO:0015934	Large ribosomal subunit	30/152	7.73×10^{-38}
GO:0022627	Cytosolic small ribosomal subunit	23/152	7.36×10^{-37}
GO:0015935	Small ribosomal subunit	23/152	3.17×10^{-31}
GO:0042788	Polysomal ribosome	18/152	1.63×10^{-30}
GO:0005844	Polysome	20/152	1.49×10^{-26}
GO:0005925	focal adhesion	31/152	8.34×10^{-22}
MF			
GO:0003735	Structural constituent of ribosome	52/149	2.62×10^{-65}
GO:0019843	rRNA binding	11/149	3.58×10^{-12}

BP, biological process; CC, cellular component; ER, endoplasmic reticulum; GO, Gene Ontology; ID, identifier; MF, molecular function; rRNA, ribosomal RNA; SRP, signal recognition particle.

achieved the highest score (score, 57.404) and featured the most hub genes.

Discussion

TACE is increasingly used in clinical settings as the primary treatment for patients with unresectable HCC, which can effectively prolong the survival of patients (5). Currently, the main tumor marker used to predict the efficacy and prognosis of TACE is AFP (14). However, there are patients with HCC with negative serum AFP levels, and it is difficult to predict the effectiveness of TACE using AFP levels in clinical practice (13). Liebman *et al* (15) first reported elevated serum DCP levels in patients with HCC in 1984 and that high-DCP levels were associated with the development, metastasis and recurrence of HCC. Since then, several studies have demonstrated that serum DCP levels are an essential factor in the prognosis of HCC (29,30), and DCP has become one of the commonly accepted serum oncology markers in clinical practice. In the Japanese Society of Hepatology clinical guidelines for HCC, DCP is included for the assessment of the diagnosis and prognosis of HCC, and the Asia-Pacific Association for the Study of the Liver also recommends testing serum DCP levels (31,32). On one hand, to the best of our knowledge, for AFP-negative patients with HCC, there are no studies that have explored the value of DCP in predicting the prognosis of patients treated by TACE (33,34). The exploration of these populations is one of the highlights of the present study. On the other hand, previous studies did not use bioinformatics to analyze 'single positive' patients. The present study briefly explored the key signaling pathways and the relevant genes.

There is a lack of reports on the relationship between DCP levels and prognosis in patients with AFP-negative HCC treated with TACE, and the molecular mechanisms of 'single positivity' remain poorly understood. Saito *et al* (33) reported a case-control study of 100 patients with HCC treated by TACE, showing that high-DCP levels before TACE were associated with poor liver function. A study of 1,560 patients with HCC treated with TACE conducted by Kinugasa *et al* (34) revealed that high-DCP levels were associated with local recurrence, with local recurrence rates of 18.6, 33.4 and 61.8% at 3 months, 6 months and 1 year, respectively, and intrahepatic distant recurrence rates. In the present study, the mortality rate in the high-DCP group (37.0%) was significantly higher than that in

Table IV. Most significantly enriched KEGG terms for differentially expressed genes determined using the Gene Expression Omnibus dataset.

KEGG pathway number	Signaling pathway	Gene ratio	P-value
Downregulated			
hsa04978	Mineral absorption	9/57	2.48×10^{-10}
hsa03320	PPAR signaling pathway	6/57	1.39×10^{-5}
hsa04610	Complement and coagulation cascades	6/57	2.66×10^{-5}
hsa00280	Valine, leucine and isoleucine degradation	4/57	3.42×10^{-4}
hsa00220	Arginine biosynthesis	3/57	4.64×10^{-4}
hsa00010	Glycolysis/Gluconeogenesis	4/57	1.22×10^{-3}
hsa01200	Carbon metabolism	5/57	1.23×10^{-3}
hsa00830	Retinol metabolism	4/57	1.29×10^{-3}
hsa01230	Biosynthesis of amino acids	4/57	1.85×10^{-3}
hsa00250	Alanine, aspartate and glutamate metabolism	3/57	2.17×10^{-3}
Upregulated			
hsa03010	Ribosome	53/64	6.65×10^{-83}
hsa05171	Coronavirus disease-COVID-19	53/64	3.55×10^{-68}

COVID-19, coronavirus disease 2019; KEGG, Kyoto Encyclopedia of Genes and Genomes; PPAR, peroxisome proliferator-activated receptor.
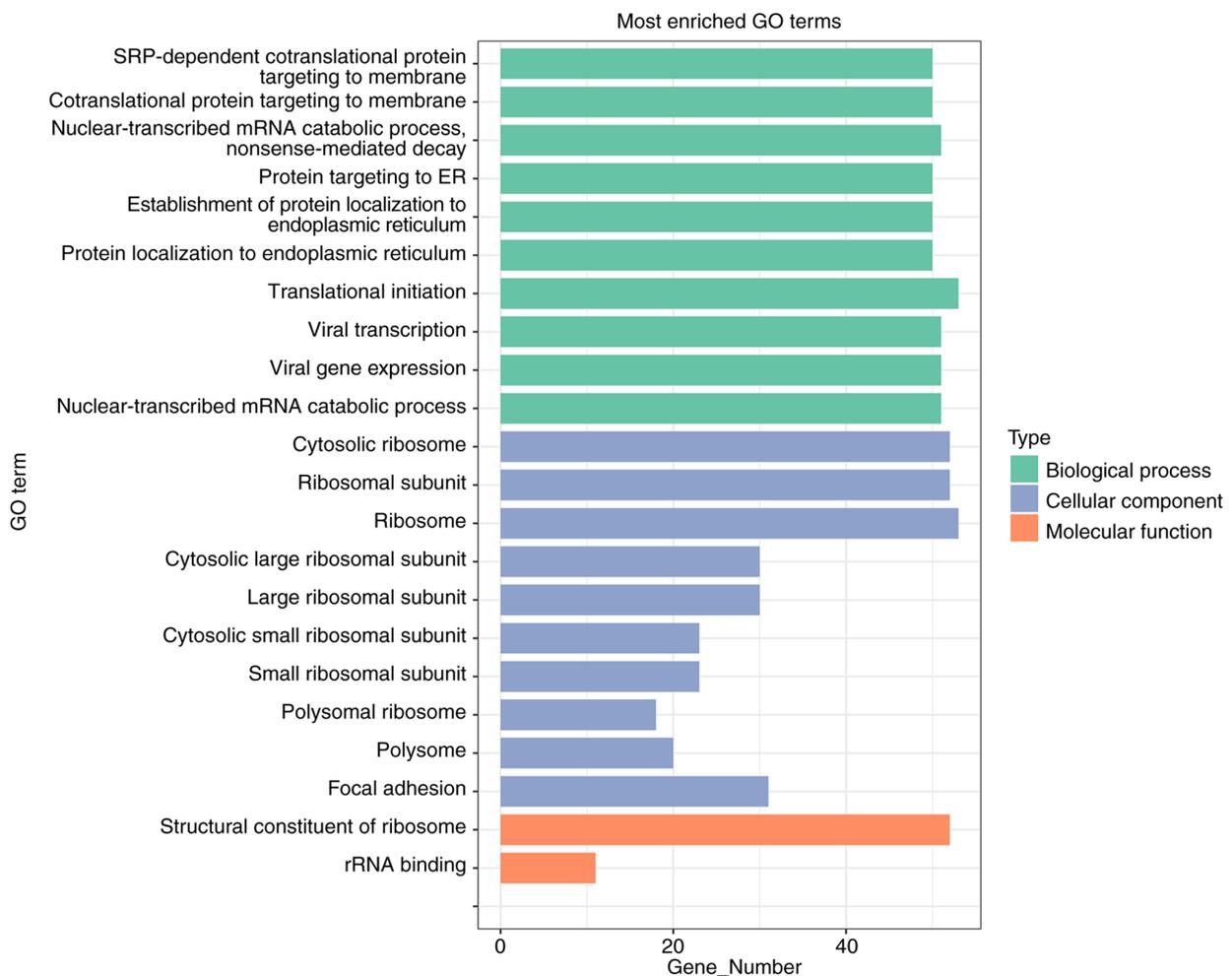

Figure 4. GO enrichment analysis of DEGs. The bar plot shows significant GO enrichment terms of DEGs in three functional groups: Molecular function, biological processes and cellular component. The x-axis indicates the gene number and the y-axis indicates the pathway. DEGs, differentially expressed genes; ER, endoplasmic reticulum; GO, Gene Ontology; mR, mRNA; rR, ribosomal RNA; SRP, signal recognition particle.
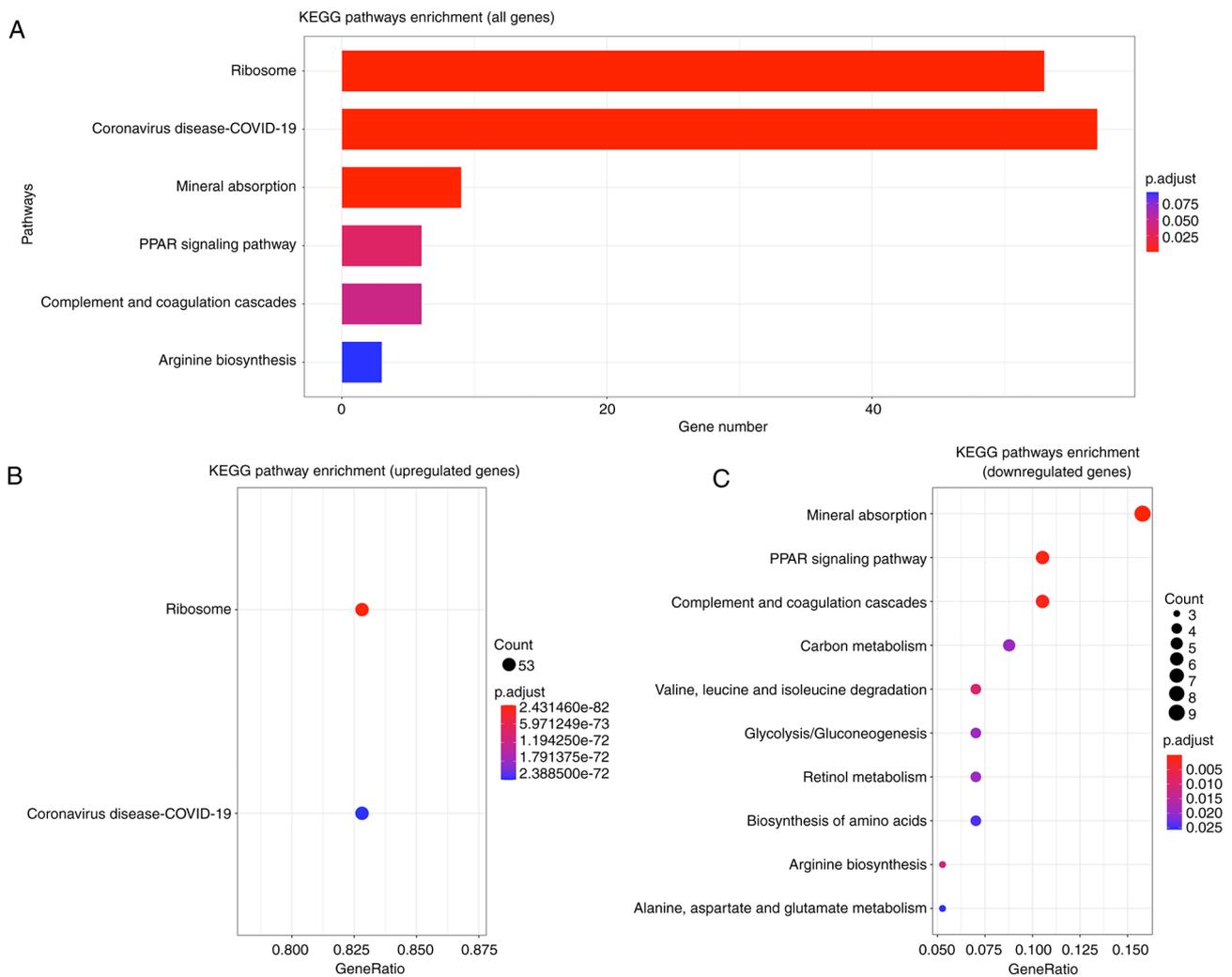
Figure 5. KEGG pathway analysis of DEGs. (A) Bar plot showing the KEGG pathway enrichment of all DEGs. The x-axis indicates the gene number and the y-axis indicates the pathway. Advanced bubble charts showing enrichment of (B) upregulated and (C) downregulated DEGs in signaling pathways. The x-axis indicates the gene ratio and the y-axis indicates the pathway. COVID-19, coronavirus disease 2019; DEGs, differentially expressed genes; KEGG, Kyoto Encyclopedia of Genes and Genomes; PPAR, peroxisome proliferator-activated receptor.

the low-DCP group (20.8%), indicating that the prognosis of patients with AFP-negative HCC can be assessed by preoperative serum DCP levels.

The present study revealed no significant association between serum DCP levels and sex, age group, hepatitis, Child-Pugh classification, AST, TBil, HDL, RBP, PLT, PDW, RDW, tumor number, lymph node metastasis or distant metastasis but a positive association with ECOG score, ALT and tumor size. The results demonstrated that the serum DCP level was an important indicator affecting the prognosis of patients with AFP-negative HCC treated by TACE, and the serum DCP level was negatively associated with prognosis, which was consistent with the results of Payancé *et al* (35). A related study found that the serum DCP level was not significantly associated with AFP, and the accuracy of the DCP level as a prognostic assessment was greater than that of AFP (36).

Microarray technology and bioinformatics analysis enable researchers to identify genetic differences between tumors and normal tissues and help discover novel biomarkers (37,38). The present study analyzed the GSE57555 gene expression profile dataset and revealed that 169 DEGs were present

in 'single-positive' patients, with significant differences compared with normal tissues, including 83 upregulated genes and 86 downregulated genes. In addition, both GO and KEGG analyses demonstrated that genes were enriched in the ribosomal pathway, suggesting that ribosome-related genes may serve a role in 'single-positive' HCC. A 'single-positive' HCC-related PPI network was also constructed and 10 hub genes were identified by centrality analysis. Notably, nine genes were from the ribosomal protein family. These results imply that ribosomal protein family genes may participate in 'single-positive' HCC.

The ribosomal protein family is the cornerstone of ribosome biogenesis and involved in the assembly of the ribosome (39). RPS23, RPS11, RPS3A, RPS2, RPS15, RPS5 and RPS13 are components of the 40S subunit, and RPL6 and RPL18 are components of the 60S subunit (39). In the present study, the top three significant genes were RPS23, RPS11 and RPS3A. Upregulation of RPS23 promotes the biogenesis of 18S ribosomal RNA, which is detrimental to the oncogenic effect of the tumor suppressor p53 (40). A high RPS11 level in HCC is associated with poor prognosis after curative resection,
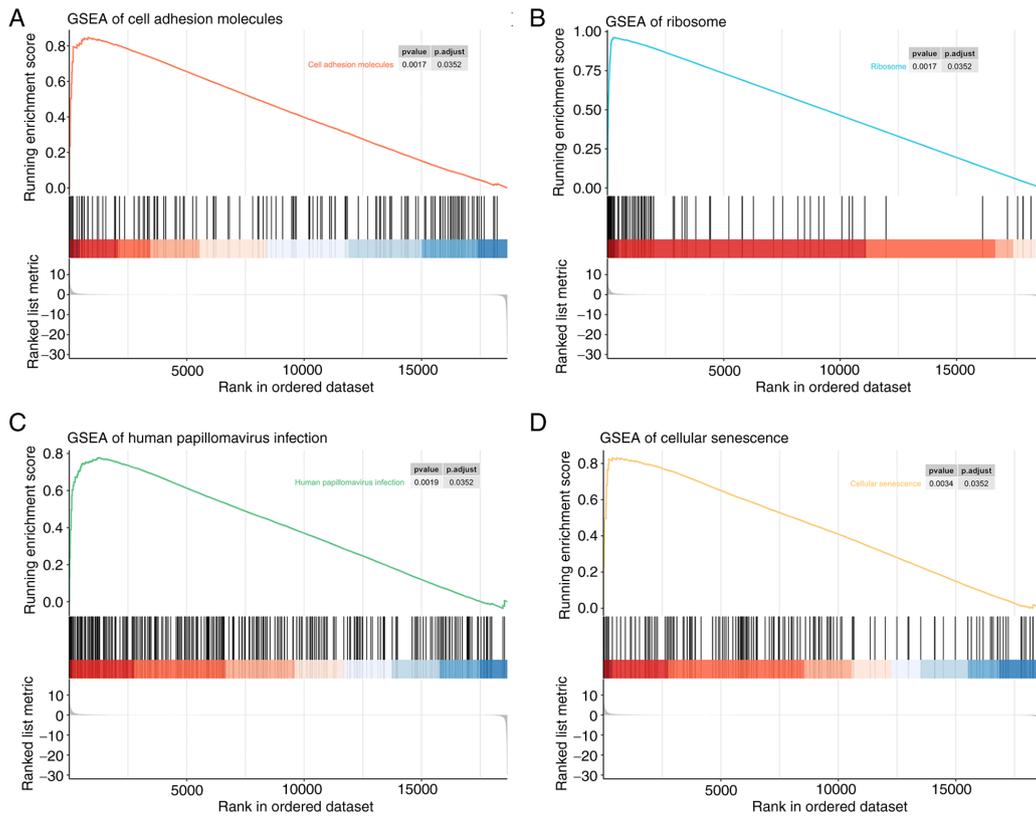
Figure 6. GSEA plots indicating the most enriched gene sets of all detected genes. The top four most significantly regulated enriched gene sets were: (A) 'Cell adhesion molecules', (B) 'Ribosome', (C) 'Human papillomavirus infection' and (D) 'Cellular senescence'. GSEA, Gene Set Enrichment Analysis.
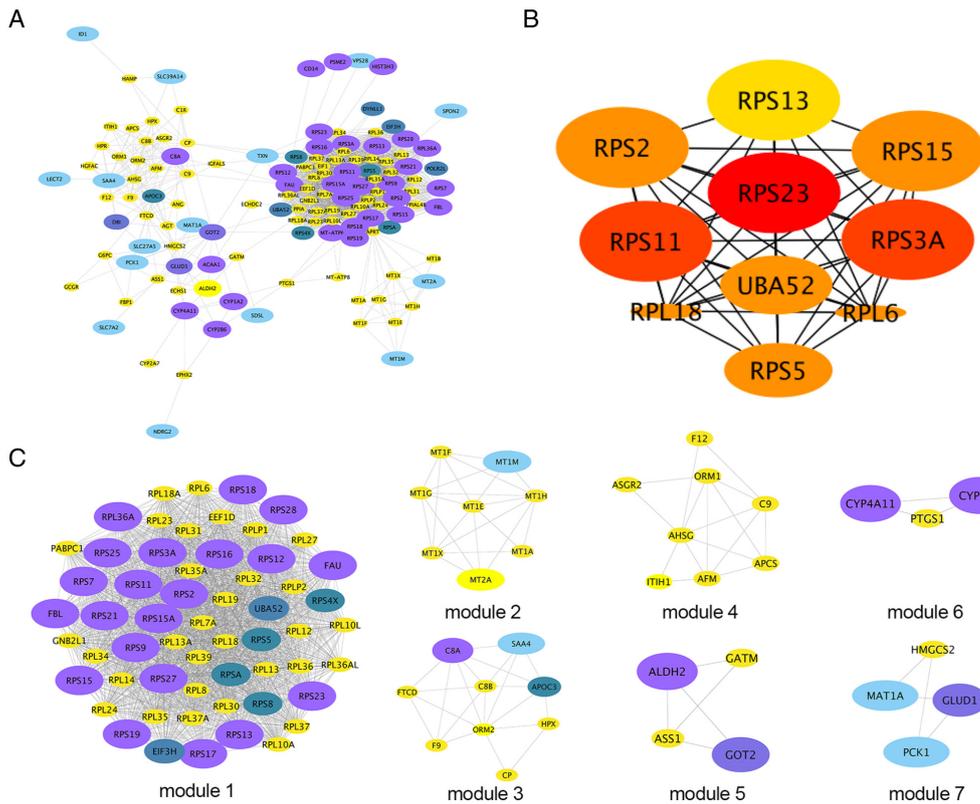

Figure 7. PPI network. (A) PPI network of DEGs. The color depth of nodes refer to the 'degree' calculated by Cytoscape (purple represents a higher degree, blue a medium degree and yellow a lower degree). (B) Subnetwork of the top 10 hub genes from the PPI network. The color of the nodes reflects the degree of connectivity of the nodes (red represents higher connectivity, and yellow represents lower connectivity). The results suggest that the top three hub genes with a higher degree of connectivity are RPS23, RPS11 and RPS3A. (C) Module analysis for aberrantly methylated DEGs. The color of nodes indicates the 'degree' (purple represents a higher degree, blue a medium degree and yellow a lower degree). DEGs, differentially expressed genes; PPI, protein-protein interaction.

suggesting a potential tumor-promoting role for RPS11 (41). In addition, high RPS3A expression is associated with low tumor immune cell infiltration and unfavorable prognosis in patients with HCC (42). In our study, 'single-positive' HCC exhibited abnormally high expression of the ribosomal protein family. Therefore, the study of ribosomal proteins may provide an important novel direction for the diagnosis, prognosis and treatment of 'single-positive' HCC.

The present study has several limitations. First, as with most retrospective studies, the study was not randomized in design, which may have led to some bias. Second, as the median follow-up period was 755 days, survival data were limited. Although the value of DCP was confirmed in predicting prognosis, further follow-up is necessary. Third, the number of patients (n=107) was relatively small, and studies involving more patients are required to further support the findings. Finally, the potential link between DCP and genes needs to be further explored in *in vivo* and *in vitro* studies.

In conclusion, the present study demonstrated that higher serum DCP levels in patients with AFP-negative HCC were associated with poor prognosis after TACE and revealed that the occurrence of 'single-positive' HCC might be associated with genes such as the ribosomal protein family. Exploration in this area will facilitate the discovery of personalized regimens for TACE treatment in patients with serum AFP-negative HCC. These genes from the RPS family may be potential diagnostic and prognostic biomarkers that could contribute to targeted treatment of the disease.

Availability of data and materials

The microarray datasets generated and/or analyzed during the current study are available in the GEO repository, https://www. ncbi.nlm.nih.gov/geo/query/acc.cgi?acc=GSE57555. All other data generated or analyzed during this study are included in this published article.

Authors' contributions

HS and WY were involved in conceptualization, project administration, formal analysis, use of software, writing and editing. WZ and CZ conceived and designed the study, and prepared figures and tables. SL collected and analyzed data. HS and WT were involved in conceptualization, supervision,

writing, review and editing. HS and WT confirm the authenticity of all the raw data. All authors read and approved the final manuscript.

Ethics approval and consent to participate

This retrospective study was discussed and approved by the ethics committee review board of Jiangsu Provincial Hospital (Nanjing, China), which waived the requirement for informed consent (approval no. 2022-SR-249).

Patient consent for publication

Not applicable.

Competing interests

The authors declare that they have no competing interests.

References

1. Villanueva A: Hepatocellular carcinoma. N Engl J Med 380: 1450-1462, 2019.
2. Llovet JM, Kelley RK, Villanueva A, Singal AG, Pikarsky E, Roayaie S, Lencioni R, Koike K, Zucman-Rossi J and Finn RS: Hepatocellular carcinoma. Nat Rev Dis Primers 7: 6, 2021.
3. Lencioni R, de Baere T, Soulen MC, Rilling WS and Geschwind JFH: Lipiodol transarterial chemoembolization for hepatocellular carcinoma: A systematic review of efficacy and safety data. Hepatology 64: 106-116, 2016.
4. Llovet JM and Bruix J: Systematic review of randomized trials for unresectable hepatocellular carcinoma: Chemoembolization improves survival. Hepatology 37: 429-442, 2003.
5. Murata S, Mine T, Sugihara F, Yasui D, Yamaguchi H, Ueda T, Onozawa S and Kumita S: Interventional treatment for unresectable hepatocellular carcinoma. World J Gastroenterol 20: 13453-13465, 2014.
6. Murakami T and Tsurusaki M: Hypervascular benign and malignant liver tumors that require differentiation from hepatocellular carcinoma: Key points of imaging diagnosis. Liver Cancer 3: 85-96, 2014.
7. Tsurusaki M and Murakami T: Surgical and locoregional therapy of HCC: TACE. Liver Cancer 4: 165-175, 2015.
8. Chen X, Tang FR, Arfuso F, Cai WQ, Ma Z, Yang J and Sethi G: The emerging role of long non-coding RNAs in the metastasis of hepatocellular carcinoma. Biomolecules 10: 66, 2019.
9. Ji J, Gu J, Wu JZ, Yang W, Shi HB, Liu S and Zhou WZ: The 'six-and-twelve' score for recurrent HCC patients receiving TACE: Does it still work? Cardiovasc Intervent Radiol 44: 720-727, 2021.
10. Bruix J, Sala M and Llovet JM: Chemoembolization for hepatocellular carcinoma. Gastroenterology 127 (5 Suppl 1): S179-S188, 2004.
11. Llovet JM, Real MI, Montaña X, Planas R, Coll S, Aponte J, Ayuso C, Sala M, Muchart J, Solà R, *et al*: Arterial embolisation or chemoembolisation versus symptomatic treatment in patients with unresectable hepatocellular carcinoma: A randomised controlled trial. Lancet 359: 1734-1739, 2002.
12. Tsuchiya N, Sawada Y, Endo I, Saito K, Uemura Y and Nakatsura T: Biomarkers for the early diagnosis of hepatocellular carcinoma. World J Gastroenterol 21: 10573-10583, 2015.
13. Luo P, Wu S, Yu Y, Ming X, Li S, Zuo X and Tu J: Current status and perspective biomarkers in AFP negative HCC: Towards screening for and diagnosing hepatocellular carcinoma at an earlier stage. Pathol Oncol Res 26: 599-603, 2020.
14. Wang T and Zhang KH: New blood biomarkers for the diagnosis of AFP-negative hepatocellular carcinoma. Front Oncol 10: 1316, 2020.
15. Liebman HA, Furie BC, Tong MJ, Blanchard RA, Lo KJ, Lee SD, Coleman MS and Furie B: Des-gamma-carboxy (abnormal) prothrombin as a serum marker of primary hepatocellular carcinoma. N Engl J Med 310: 1427-1431, 1984.

16. Inagaki Y, Tang W, Makuuchi M, Hasegawa K, Sugawara Y and Kokudo N: Clinical and molecular insights into the hepatocellular carcinoma tumour marker des-γ-carboxyprothrombin. Liver Int 31: 22-35, 2011.
17. Verslype C, Rosmorduc O and Rougier P; ESMO Guidelines Working Group: Hepatocellular carcinoma: ESMO-ESDO clinical practice guidelines for diagnosis, treatment and follow-up. Ann Oncol 23 (Suppl 7): vii41-vii48, 2012.
18. Oken MM, Creech RH, Tormey DC, Horton J, Davis TE, McFadden ET and Carbone PP: Toxicity and response criteria of the eastern cooperative oncology group. Am J Clin Oncol 5: 649-655, 1982.
19. Seldinger SI: Catheter replacement of the needle in percutaneous arteriography; a new technique. Acta Radiol 39: 368-376, 1953.
20. Zhou J, Sun H, Wang Z, Cong W, Wang J, Zeng M, Zhou W, Bie P, Liu L, Wen T, et al: Guidelines for the diagnosis and treatment of hepatocellular carcinoma (2019 edition). Liver Cancer 9: 682-720, 2020.
21. Laird BJ, Kaasa S, McMillan DC, Fallon MT, Hjermstad MJ, Fayers P and Klepstad P: Prognostic factors in patients with advanced cancer: A comparison of clinicopathological factors and the development of an inflammation-based prognostic system. Clin Cancer Res 19: 5456-5464, 2013.
22. Barrett T, Wilhite SE, Ledoux P, Evangelista C, Kim IF, Tomashevsky M, Marshall KA, Phillippy KH, Sherman PM, Holko M, et al: NCBI GEO: Archive for functional genomics data sets-update. Nucleic Acids Res 41 (Database Issue): D991-D995, 2013.
23. Murakami Y, Kubo S, Tamori A, Itami S, Kawamura E, Iwaisako K, Ikeda K, Kawada N, Ochiya T and Taguchi YH: Comprehensive analysis of transcriptome and metabolome analysis in intrahepatic cholangiocarcinoma and hepatocellular carcinoma. Sci Rep 5: 16294, 2015.
24. Diboun I, Wernisch L, Orengo CA and Koltzenburg M: Microarray analysis after RNA amplification can detect pronounced differences in gene expression using limma. BMC Genomics 7: 252, 2006.
25. Ashburner M, Ball CA, Blake JA, Botstein D, Butler H, Cherry JM, Davis AP, Dolinski K, Dwight SS, Eppig JT, et al: Gene ontology: Tool for the unification of biology. The gene ontology consortium. Nat Genet 25: 25-29, 2000.
26. Szklarczyk D, Morris JH, Cook H, Kuhn M, Wyder S, Simonovic M, Santos A, Doncheva NT, Roth A, Bork P, et al: The STRING database in 2017: Quality-controlled protein-protein association networks, made broadly accessible. Nucleic Acids Res 45 (D1): D362-D368, 2017.
27. Chin CH, Chen SH, Wu HH, Ho CW, Ko MT and Lin CY: cyto-Hubba: Identifying hub objects and sub-networks from complex interactome. BMC Syst Biol 8 (Suppl 4): S11, 2014.
28. Bader GD and Hogue CWV: An automated method for finding molecular complexes in large protein interaction networks. BMC Bioinformatics 4: 2, 2003.
29. Lee YK, Kim SU, Kim DY, Ahn SH, Lee KH, Lee DY, Han KH, Chon CY and Park JY: Prognostic value of α-fetoprotein and des-γ-carboxy prothrombin responses in patients with hepatocellular carcinoma treated with transarterial chemoembolization. BMC Cancer 13: 5, 2013.
30. Hiraoka A, Ishimaru Y, Kawasaki H, Aibiki T, Okudaira T, Toshimori A, Kawamura T, Yamago H, Nakahara H, Suga Y, et al: Tumor markers AFP, AFP-L3, and DCP in hepatocellular carcinoma refractory to transcatheter arterial chemoembolization. Oncology 89: 167-174, 2015.
31. Kokudo N, Hasegawa K, Akahane M, Igaki H, Izumi N, Ichida T, Uemoto S, Kaneko S, Kawasaki S, Ku Y, et al: Evidence-based clinical practice guidelines for hepatocellular carcinoma: The Japan society of hepatology 2013 update (3rd JSH-HCC guidelines). Hepatol Res 45, 2015.
32. Omata M, Lesmana LA, Tateishi R, Chen PJ, Lin SM, Yoshida H, Kudo M, Lee JM, Choi BI, Poon RT, et al: Asian pacific association for the study of the liver consensus recommendations on hepatocellular carcinoma. Hepatol Int 4: 439-474, 2010.
33. Saito M, Seo Y, Yano Y, Miki A, Yoshida M and Azuma T: A high value of serum des-γ-carboxy prothrombin before hepatocellular carcinoma treatment can be associated with long-term liver dysfunction after treatment. J Gastroenterol 47: 1134-1142, 2012.
34. Kinugasa H, Nouso K, Takeuchi Y, Yasunaka T, Onishi H, Nakamura S, Shiraha H, Kuwaki K, Hagihara H, Ikeda F, et al: Risk factors for recurrence after transarterial chemoembolization for early-stage hepatocellular carcinoma. J Gastroenterol 47: 421-426, 2012.
35. Payancé A, Dioguardi Burgio M, Peoc'h K, Achahboun M, Albuquerque M, Devictor J, Chor H, Manceau H, Soubrane O, Durand F, et al: Biological response under treatment and prognostic value of protein induced by vitamin K absence or antagonist-II in a French cohort of patients with hepatocellular carcinoma. Eur J Gastroenterol Hepatol 32: 1364-1372, 2020.
36. Yamamoto K, Imamura H, Matsuyama Y, Hasegawa K, Beck Y, Sugawara Y, Makuuchi M and Kokudo N: Significance of alpha-fetoprotein and des-gamma-carboxy prothrombin in patients with hepatocellular carcinoma undergoing hepatectomy. Ann Surg Oncol 16: 2795-2804, 2009.
37. Vogelstein B, Papadopoulos N, Velculescu VE, Zhou S, Diaz LA Jr and Kinzler KW: Cancer genome landscapes. Science 339: 1546-1558, 2013.
38. Guo Y, Bao Y, Ma M and Yang W: Identification of key candidate genes and pathways in colorectal cancer by integrated bioinformatical analysis. Int J Mol Sci 18: 722, 2017.
39. Warner JR and McIntosh KB: How common are extraribosomal functions of ribosomal proteins? Mol Cell 34: 3-11, 2009.
40. Wang Y, Huang JW, Castella M, Huntsman DG and Taniguchi T: p53 is positively regulated by miR-542-3p. Cancer Res 74: 3218-3227, 2014.
41. Zhou C, Sun J, Zheng Z, Weng J, Atyah M, Zhou Q, Chen W, Zhang Y, Huang J, Yin Y, et al: High RPS11 level in hepatocellular carcinoma associates with poor prognosis after curative resection. Ann Transl Med 8: 466, 2020.
42. Zhou C, Weng J, Liu C, Zhou Q, Chen W, Hsu JL, Sun J, Atyah M, Xu Y, Shi Y, et al: High RPS3A expression correlates with low tumor immune cell infiltration and unfavorable prognosis in hepatocellular carcinoma patients. Am J Cancer Res 10: 2768-2784, 2020.